Journal of Biomedical Optics 6(1), 31–40 (January 2001)

Autofluorescence characteristics of immortalized and carcinogen-transformed human bronchial epithelial cells

Jonathan D. Pitts
Dartmouth College
Department of Physics and Astronomy
Norris Cotton Cancer Center
Hanover, New Hampshire 03755

Roger D. Sloboda
Dartmouth College
Department of Biological Sciences
Norris Cotton Cancer Center
Hanover, New Hampshire 03755

Konstantin H. Dragnev
Dartmouth Medical School
Department of Medicine
Dartmouth–Hitchcock Medical Center
Norris Cotton Cancer Center
Hanover, New Hampshire 03755

Ethan Dmitrovsky
Dartmouth Medical School
Department of Pharmacology and Toxicology
and Department of Medicine
and
Dartmouth–Hitchcock Medical Center
Norris Cotton Cancer Center
Hanover, New Hampshire 03755

Mary-Ann Mycek
Dartmouth College
Department of Physics and Astronomy
and
Dartmouth–Hitchcock Medical Center
Norris Cotton Cancer Center
Hanover, New Hampshire 03755

Abstract. Tissue autofluorescence has been explored as a potential method of noninvasive pre-neoplasia (pre-malignancy) detection in the lung. Here, we report the first studies of intrinsic cellular autofluorescence from SV40 immortalized and distinct tobacco-carcinogen-transformed (malignant) human bronchial epithelial cells. These cell lines are useful models for studies seeking to distinguish between normal and pre-neoplastic human bronchial epithelial cells. The cells were characterized via spectrofluorimetry and confocal fluorescence microscopy. Spectrofluorimetry revealed that tryptophan was the dominant fluorophore. No change in tryptophan emission intensity was observed between immortalized and carcinogen-transformed cells. Confocal autofluorescence microscopy was performed using a highly sensitive, spectrometer-coupled instrument capable of limiting emission detection to specific wavelength ranges. These studies revealed two additional endogenous fluorophores, whose excitation and emission characteristics were consistent with nicotinamide adenine dinucleotide (NADH) and flavins. In immortalized human bronchial epithelial cells, the fluorescence of these species was localized to cytoplasmic granules. In contrast, the carcinogen-transformed cells showed an appreciable decrease in the fluorescence intensity of both NADH and flavins and the punctate, spatial localization of the autofluorescence was lost. The observed autofluorescence decrease was potentially the result of changes in the redox state of the fluorophores. The random cytoplasmic fluorescence pattern found in carcinogen-transformed cells may be attributed to changes in the mitochondrial morphology. The implications of these results to pre-neoplasia detection in the lung are discussed. [DOI: 10.1117/1.1333057]

Keywords: fluorescence spectroscopy; cellular autofluorescence; bronchial epithelial cells; confocal microscopy; lung cancer detection; tobacco-carcinogen transformation.

Paper JBO 20022 received June 5, 2000; revised manuscript received Oct. 9, 2000; accepted for publication Oct. 11, 2000.

1 Introduction

Human tissue autofluorescence spectroscopy and imaging are being explored as potential methods of noninvasive disease diagnosis.[1–4] Autofluorescence studies on *in vivo* and *ex vivo* human tissues include the cervix,[5–9] bladder,[10–12] lung,[13–18] breast,[18–21] esophagus,[22–24] aorta,[25] stomach,[26] uterus,[27] skin,[28–32] and colon.[33–41] Tissue autofluorescence contains contributions from endogenous cellular and extracellular biomolecular species, and is influenced by light absorption and scattering, making detailed physical interpretations difficult. Studies on isolated cells in culture should help determine what portion of the tissue fluorescence arises from intrinsic cellular components. This understanding may, in turn, advance the application of autofluorescence methods to noninvasive diagnosis of human neoplastic disease.

Several endogenous cellular fluorophores have been reported in the literature.[1] One of the most studied is the reduced form of nicotinamide adenine dinucleotide (NADH).[42–44] This reduced coenzyme typically has an excitation maximum near 380 nm and an emission maximum near 440 nm. Contributions from flavins (FAD, FMN, and riboflavin) are often observed in cellular autofluorescence.[42–45] Their steady-state fluorescence characteristics show an excitation maximum near 450 nm and an emission maximum near 515 nm. Lipofuscin granules are age-related lipophylic materials composed primarily of malonaldehyde.[46–48] These pigments absorb between 340 and 395 nm and emit in the red region of the electromagnetic spectrum (up to 640 nm).[1,2,49] Another known endogenous cellular fluorophore is the amino acid tryptophan. Tryptophan has two absorption bands observed at

Address all correspondence to Professor Mary-Ann Mycek, Department of Physics and Astronomy, 6127 Wilder Laboratory, Hanover, NH 03755. Voice: (603) 646-2738; Fax: (603) 646-1446; E-mail: Mary-Ann. Mycek@Dartmouth.edu

1083-3668/2001/$15.00 © 2001 SPIE

220 and 287 nm, which emit coincidently at 350 nm.[50–53]

Over the past decade, several studies have characterized the autofluorescence properties of human epithelial cells. These cells are of interest, because carcinoma, the most common form of human cancer, derive from epithelial cells. In one report, both steady-state and time-resolved fluorescence spectroscopies were employed to measure unspecified epithelial cell autofluorescence.[43] Under laser excitation, fluorescence emission and discrete lifetimes attributed to endogenous NADH and flavins were detected. Using confocal microscopy, the study detected increases in cellular autofluorescence due to formalin and aminolevulinic acid treatment. It was the conclusion of the study that the fluorescence properties monitored in these cells might be useful as a diagnostic tool to detect neoplastic changes. In another study, human oral epithelial cells (explanted from the normal mucosa of the tonsillar pillar) were monitored to determine if autofluorescence could differentiate between slowly growing (treated with TGF-β) and rapidly growing (untreated) cells.[54] It was found that changes in endogenous NADH fluorescence discriminated between different proliferation rates. A subsequent report indicated that autofluorescence signatures might be useful in distinguishing between benign (normal) and malignant (squamous carcinoma line, 1483) oral epithelial cells.[55] This study detected spectral shifts, as well as changes in autofluorescence intensity between cell types. The observed differences between normal and malignant cell emission spectra were attributed to changes in the optical absorption of residues such as tyrosine, tryptophan, phenylalanine, and others. Autofluorescence of epithelial cells from the human larynx, both squamous cell carcinoma (Hep_2) and nontumorigenic (Vero) lines, have also been reported.[56] This investigation observed autofluorescence emission at 340 and 440 nm that might be useful as a marker of malignancy or for uncovering mechanisms linked to transformation of epithelial cells. Recent studies monitored the autofluorescence from human epithelial cervical cancer lines (HeLa and SiHa), and found tryptophan, NADH, and FAD to be the primary fluorophores.[57–59]

Autofluorescence from bronchial tissue has been investigated as a means of lung cancer detection.[13–18,60–69] Currently, a FDA approved fluorescence imaging device for the lung relies upon autofluorescence properties to detect intraepithelial neoplastic lesions.[16] While there are prior reports of tissue autofluorescence, there are few prior studies of isolated bronchial epithelial cell autofluorescence. One such study recently reported in the literature[70] measures human bronchial cell autofluorescence from a single sample, and will be discussed later. An important motivation for the work presented here, is to thoroughly investigate well-characterized cellular models, which may help to interpret the results of tissue studies. In this report, we describe the first study on the autofluorescence characteristics of both an immortalized and a distinct tobacco-carcinogen-transformed human bronchial epithelial cell line. These cell lines are useful models for studies seeking to distinguish between normal and transformed human bronchial epithelial cells. The goal of this work is to characterize the autofluorescence spectra of these cellular models. Spectrofluorimetry and confocal fluorescence microscopic imaging were employed to determine the predominant contributors to the observed cellular autofluorescence patterns and to compare differences in autofluorescence between the immortalized and carcinogen-transformed phenotypes. To date, such an investigation on these cell lines has not been reported.

2 Experiment

2.1 Human Bronchial Epithelial Cell Lines

The cells studied were previously described and included a line (designated BEAS-2B) derived from normal human bronchial epithelial cells that was immortalized via transduction of the SV40 T antigen.[71] Another line (designated $BEAS\text{-}2B_{NNK}$) was derived through tobacco-carcinogen-induced transformation of BEAS-2B cells following treatment with N-nitrosamine-4-(methylnitrosamino)-1-(3-pyridyl)-1-butanone (NNK).[72] BEAS-2B cells retain features of normal human bronchial epithelial cells, but can be continuously passed *in vitro*. The tobacco-carcinogen-transformed $BEAS\text{-}2B_{NNK}$ line has acquired characteristics of malignant bronchial epithelial cells including tumorigenicity in athymic mice and enhanced anchorage-independent growth.[72] These cell lines have proven useful for identifying carcinogenic and anticarcinogenic pathways.[72–75] These lines represent valuable models for studies seeking to distinguish between immortalized and transformed human bronchial epithelial cells.

For cell suspension studies, monolayer cultures maintained in a chemically defined medium, LHC-9, (Biofluids, Rockville, MD) at 37°C and 5% CO_2, were trypsinized (0.05%) for 4 min, diluted in medium, and centrifuged for 4 min. Upon removal of the medium, cells were washed and resuspended in phosphate-buffered saline (PBS), before being placed in a 1 cm quartz cuvette. All measurements were made in less than 1 h after resuspension to preserve cell viability. Viability limits were determined by measuring the occurrence of fluorescence changes over time. These changes were found to be negligible within this 1 h period.

For imaging experiments, nonconfluent monolayers of cells were prepared on standard cover slips by plating cells 24 h prior to imaging. For each cell line, three independent cell cultures were maintained. From each culture, a minimum of two glass cover slips were used. The cover slips were moved from the incubator directly to the microscope, where multiple measurements were taken. All images were taken in culture medium. Visual inspection demonstrated that the presence of media increased the viability of the cells to greater than 1 h. No sample was imaged for more than 45 min.

2.2 Spectrofluorimetry

Spectrofluorimetry measurements were performed on the model systems described above to characterize their autofluorescence properties. A Perkin–Elmer LS-50 dual monochromator luminescence spectrometer was used for fluorescence measurements throughout the ultraviolet, visible, and near-infrared regions of the electromagnetic spectrum. The instrument contained a xenon arc-discharge lamp as an excitation light source and a red-enhanced photomultiplier tube (Hamamatsu R928), with an extended range of 200–900 nm, as an emission detector. Emission was collected at a 90° angle relative to the excitation light path. The wavelength accuracy of the instrument was ± 1.0 nm, and the reproducibility was ± 0.5 nm. All spectra were corrected for solvent contributions, by background subtraction of a prerecorded solvent emission, and for the nonuniformity of the instrument

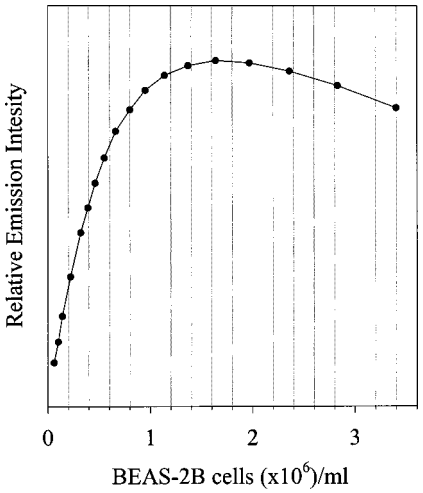

Fig. 1 Maximum emission intensity of a band consistent with tryptophan (excitation at 287 nm), collected on the LS-50 spectrofluorimeter, as a function of BEAS-2B cell number. A nearly linear emission intensity trend was observed for counts $<$ 500 000 cells/ml. Beyond this range, reabsorption and scattering artifacts affect emission intensities. Error associated with the data points arose primarily from cell-counting techniques and was estimated to be as much as 10%–20% of the cell number.

response, by division of a wavelength-dependent sensitivity factor.[50] These sensitivity factors were previously obtained, for this spectrometer, by recording the fluorescence emission of quinine sulfate (0.1 N) and forming the ratio with the known standard spectrum. Equation (1) describes the spectral correction procedure:

$$\text{corrected emission} = \frac{M(\lambda) - B(\lambda)}{S(\lambda)}, \qquad (1)$$

where $M(\lambda)$ is the measured sample emission and $B(\lambda)$ and $S(\lambda)$ are the background and sensitivity factors. Photobleaching of the cell suspension was not observed, as determined by rescanning several spectra at the completion of each experiment. All measurements were made a minimum of three times, using new cell cultures each time.

Importantly, we found that high cell counts can lead to appreciable spectral artifacts, including intrusive harmonic peaks and intensity fluctuations. The origin of these artifacts is presumably due to increased scattering of the excitation light as well as increased reabsorption of the fluorescence emission.[50] Therefore, to determine an acceptable cell count range for recording fluorescence spectra, we measured the BEAS-2B emission intensity (of a band consistent with the amino acid tryptophan) as a function of the cell number density. The results of this study are shown in Figure 1. For cell counts ranging from 60 000 to approximately 500 000 per milliliter, the emission intensity increased nearly linearly. Beyond this range, the curve deviated from this trend, presumably due to reabsorption and scattering effects. While the observed linearity in the 60 000–500 000 cells per milliliter region was not perfect, the spectra recorded in this range were sufficiently free from the spectral artifacts noted at higher cell counts. The source of deviation from linearity arises from both the above-mentioned effects and error associated with cell counting. For the experiments reported here, cell counts were consistently held at a level of approximately 300 000 cells/ml, as determined by hemocytometry.

2.3 Confocal Fluorescence Microscopy

Fluorescence imaging experiments were performed on a Leica confocal spectrophotometer (model TCS SP) equipped with an upright Leica research microscope and the necessary optics for differential interference contrast (DIC) and conventional epi-illumination. The images presented here were collected with a 63×, 1.32 NA planapochromatic objective and a 0.9 NA condenser. The confocal system employed fiber-coupled UV, argon, krypton–argon, and helium–neon lasers, providing excitation sources at wavelengths of 351, 364, 488, 514, 568, and 633 nm. Imaging occurred via transmitted and fluorescent light detection, the latter via a tunable spectrophotometer instead of filter cubes. The continuously variable spectrophotometer allowed the user to determine the emission spectrum of a given fluorescent signal and to limit fluorescence collection to a precise emission range. This feature ensured that autofluorescence from living cells could be selectively scanned to identify the contributing wavelengths and that accurate fluorophore specific images could be obtained. For the images presented here, cells were excited sequentially with two wavelengths (351 and 488 nm), rather than simultaneously, thus eliminating potential signal crossover between recording channels. The emission wavelength ranges detected were 426–454 nm, while exciting with 351 and 530–555 nm, while exciting with 488 nm. The microscope, laser, spectrophotometer, image capture, and analysis all were under computer control.

We note that the presence of the culture media did not add appreciable background to the autofluorescence images, as determined by comparison to imaging cells washed in PBS. This was presumably due to the low quantum yield of the medium at the excitation and emission wavelengths used, coupled with the inherent reduction in background from confocal sectioning. For image comparisons, experimental conditions including radiation exposure, scan rate, sample preparation, and sample temperature, were held constant. We were not able to monitor laser power directly at the sample, thus making quantitative comparisons difficult. Nonetheless, to minimize these limitations, and to make reasonable qualitative comparisons, images were acquired within the shortest time possible of each other, and no sample was used for more than 45 min.

3 Results

3.1 Spectrofluorimetry

As discussed in the experimental spectrofluorimetry section, cell counts were held at approximately 300 000 cells per milliliter. This had the result of minimizing scattering and reabsorption artifacts in the fluorescence measurements, see Figure 1. The spectrofluorimeter measurements described above were used to record the excitation/emission matrices (EEMs) of BEAS-2B and BEAS-2B$_{NNK}$ cell suspensions, as shown in Figure 2. Excitation wavelengths were chosen approximately every 20 nm and ranged from 220 to 675 nm. Emission wavelengths ranged from 10 nm beyond the excitation wavelength to 800 nm. Artifacts from grating harmonics and/or ghosts were removed from the recorded data.[76] The maximum inten-

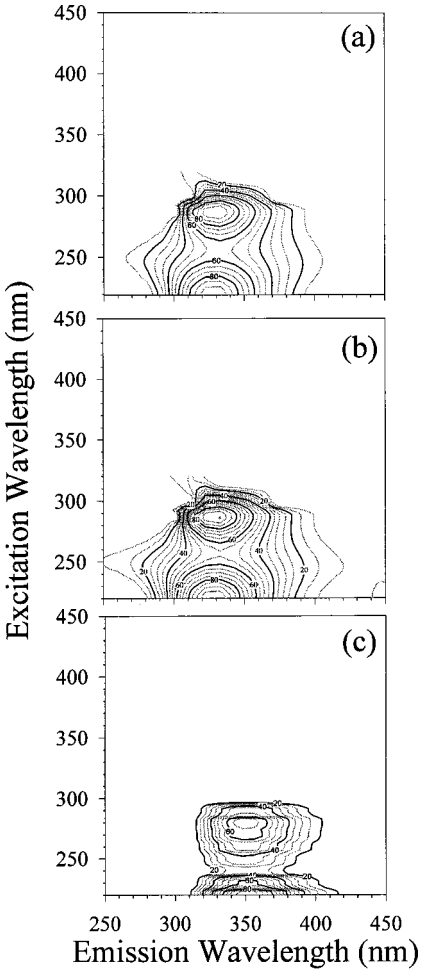

Fig. 2 EEMs of (a) BEAS-2B cells, (b) BEAS-2B$_{NNK}$ cells, and (c) pure tryptophan in PBS. Spectra were collected for excitation wavelengths from 220 to 675 nm and emission wavelengths to 800 nm. The dominant feature in both immortalized and tobacco-carcinogen-transformed cells EEMs corresponded closely to the tryptophan EEM.

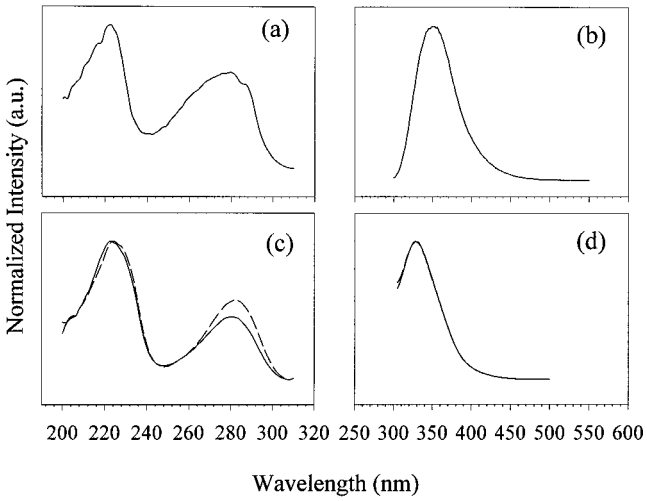

Fig. 3 (a) Excitation spectrum of pure tryptophan in PBS, emission wavelength at 350 nm. (b) Emission spectrum of pure tryptophan in PBS, excitation wavelength at 287 nm. (c) Excitation spectra of BEAS-2B cells in PBS (solid) and BEAS-2B$_{NNK}$ cells in PBS (dashed), emission wavelength at 330 nm. (d) Emission spectra of BEAS-2B cells in PBS (solid) and BEAS-2B$_{NNK}$ cells in PBS (dashed), excitation at 287 nm.

sities of the EEMs have been normalized for comparison and the wavelengths limited for presentation clarity. Two dominant peaks were observed in both the BEAS-2B [Figure 2(a)] and BEAS-2B$_{NNK}$ [Figure 2(b)] cells. These two peaks occurred at 220/330 and 287/330 nm (excitation/emission wavelengths). These peaks corresponded closely with the peaks observed in the EEM of pure tryptophan (220/350 and 287/350 nm), shown in Figure 2(c), and to those presented in the literature.[50] The peak at longer-wavelength excitation is reported to be the result of two closely spaced levels, the ^1L_a and ^1L_b of the indole moiety, while the shorter-wavelength peak is the result of a higher electronic transition.[50]

Figure 3 shows excitation and emission spectra for pure tryptophan in PBS [Figures 3(a) and 3(b)] and BEAS-2B (solid) and BEAS-2B$_{NNK}$ (dashed) cells in PBS [Figures 3(c) and 3(d)]. The spectra were recorded at the maxima of emission or excitation, as determined by the corresponding EEM. The autofluorescence spectra recorded from both bronchial epithelial cell lines closely resembled the characteristic fluorescence of the amino acid tryptophan.

A minor autofluorescence feature observed in both the BEAS-2B and BEAS-2B$_{NNK}$ cell suspensions was observed with an emission maximum at 655 nm, upon excitation at 460 nm. This broad featureless emission (full width at half maximum of 150 nm) was approximately 40 times weaker than that from the emission band at 330 nm [see the peaks in Figures 2(a) and 2(b)]. To investigate the origin of this emission, the excitation spectrum was recorded (610 nm emission) between 325 and 600 nm. This range was chosen based on values expected for porphyrins and lipofuscin, two possible endogenous fluorophores roughly corresponding to the observed emission.[2] No distinct excitation feature corresponding to reported endogenous fluorophores was found in this range. Further studies on these very small signals are needed to assign the emission observed at 655 nm.

No appreciable difference in autofluorescence emission intensity was noted between the BEAS-2B and BEAS-2B$_{NNK}$ human bronchial epithelial cells, for either the tryptophan or the 655 nm band. In addition, spectrofluorimetry revealed no emission from other common endogenous fluorophores, such as NADH and flavins. This was presumably due to the low sensitivity of the LS-50 spectrofluorimeter. In recent studies on human cervical epithelial cell suspensions, tryptophan emission was found to be at least two orders of magnitude higher than the fluorescence emission from either NADH or FAD.[59] To measure the weaker emission of other endogenous cellular fluorophores, we employed sensitive confocal fluorescence imaging methods, described next.

3.2 Confocal Fluorescence Microscopy

Using the Leica confocal microscope described above, we measured the autofluorescence of individual BEAS-2B and BEAS-2B$_{NNK}$ cells. This highly sensitive spectrophotometer-coupled instrument allowed for the detection and spatial localization of distinct fluorophore species and excluded any

appreciable contribution from other species, via tunable wavelength discrimination. Figure 4 shows two differential interference contrast (DIC) images of BEAS-2B cells, with corresponding overlays of pseudocolor confocal fluorescence images. The images in Figure 4(a) were collected using an excitation wavelength of 351 nm and emission intensity integration between 426 and 454 nm. The images revealed granular cytoplasmic autofluorescent structures with excitation/emission characteristics that corresponded closely with known NADH values. Figure 4(b) shows the same cells excited at 488 nm, with the resulting emission integrated between 530 and 555 nm. The emission in this wavelength range was consistent with the presence of flavins in the cells. From these images, it is apparent that the instrument was capable of detecting emission from these weakly fluorescing endogenous species present in human bronchial epithelial cells. Attempts at recording emission at wavelengths greater than 610 nm (488 nm excitation wavelength) were unsuccessful.

Confocal autofluorescence images comparing BEAS-2B and BEAS-2B$_{NNK}$ cells are shown in Figure 5. Figure 5 shows emission consistent with both NADH (excitation wavelength at 351 nm, emission integrated between 426 and 454 nm) and flavins (excitation wavelength at 488 nm, emission integrated between 530 and 555 nm) for the (a) BEAS-2B and (b) BEAS-2B$_{NNK}$ cells. DIC images of the corresponding fields are shown at the bottom of Figure 5, for reference. All microscope and laser parameters were held constant between corresponding images, which were acquired within minutes of one another. New areas were imaged on each sample to avoid photobleaching, and optical sections were chosen to be similar by focusing on nucleoli. These images indicate that the tobacco-carcinogen-transformed BEAS-2B$_{NNK}$ cells exhibited reduced NADH and flavin emission as compared to the immortalized BEAS-2B human bronchial epithelial cells. In addition, the punctate cytoplasmic fluorescent granules present in the immortalized cells appeared to be more dispersed in the carcinogen-transformed cells than in parental BEAS-2B cells. The microscopy system's configuration did not permit direct measurements of the excitation laser intensity or fluorescence emission intensity at the sample. This prevented any comparison between the relative NADH and flavin fluorescence intensity *in situ*.

4 Discussion

To our knowledge, this study was the first investigation of the autofluorescence characteristics of immortalized BEAS-2B and the carcinogen-transformed BEAS-2B$_{NNK}$ human bronchial epithelial cells. These cells serve as models for studies seeking to distinguish between immortalized and transformed (malignant) human bronchial epithelial cells.[72–74] The utility of this model system has been noted previously in the literature. For example, studies have used these cell lines to monitor responses to chemopreventive agents such as retinoids.[72–74] Since BEAS-2B$_{NNK}$ cells were derived from BEAS-2B cells after carcinogenic transformation, it is possible to make direct comparisons between these two cell lines. This has led to the identification of a chemopreventive pathway that affects cell cycle progression at G1.[73,74] Based on these findings, it was hypothesized that aberrant expression of these cyclins would occur in bronchial pre-neoplasia. This hypothesis has been recently confirmed.[75] Thus, these cellular models may reflect closely changes that occur during lung carcinogenesis *in vivo*.

The spectrofluorimetric results suggested that the predominant emission from both the BEAS-2B and BEAS-2B$_{NNK}$ cells arose from tryptophan residues. Figures 2 and 3 showed that pure tryptophan emission was at approximately 350 nm, while that of the cells was shifted by 20 nm to shorter wavelengths (higher energies). Similar shifts have been noted in proteins[38] and human laryngeal epithelial cells.[56] In both of these studies, a shift of approximately 10 nm to shorter wavelengths, relative to free tryptophan, was observed. Our observations agreed with these previous studies, and found that the shifts occurred in both the immortalized and the carcinogen-transformed human bronchial epithelial cells. This well-known shift is the result of changes in the local chemical environment and conformational conditions of the protein-bound tryptophan, relative to the free amino acid.[50,77] Shifts to higher energy result from orientation constraints of the amino acid, since limited molecular rearrangement subsequently raises dipole interaction energies.[50]

In general, the use of endogenous cellular fluorescence to discriminate between normal and malignant cells relies on monitoring changes in fluorescence characteristics. Two studies that were specific to human oral epithelial cells found little or no change in the emission attributed to tryptophan.[55,78] In contrast, a study on human laryngeal cells reported a decrease in the longer-wavelength edge of the tryptophan emission of malignant cells relative to nontumorigenic cells.[56] For the human bronchial epithelial cells studied here, we did not observe any change in tryptophan excitation or emission fluorescence between immortalized and carcinogen-transformed cells (Figures 2 and 3).

We note that the much weaker emission band centered at 655 nm was highly reproducible in the two human bronchial epithelial cell lines studied. The origins of this band are unknown, as are emission peaks observed in other cell types.[58] Further investigations concerning this emission band will be the subject of future work.

Confocal fluorescence imaging was used to measure weak autofluorescence contributors undetected by spectrofluorimetry and to study the spatial localization of these fluorophores in individual cells. Here, we report an appreciable decrease in the NADH autofluorescence signal of the tobacco-carcinogen-transformed BEAS-2B$_{NNK}$ cells relative to BEAS-2B cells (Figure 5). Although detailed findings have varied depending on cell type and fluorophore monitored, previous studies have reported generally less tryptophan, NADH, and/or flavin autofluorescence emission from malignant cells than from normal cells.[45,56,79,80] For example, a decrease in NADH autofluorescence was observed in malignant human laryngeal epithelial cells relative to nontumorigenic human laryngeal epithelial cells.[56] It has been suggested that the reduction in NADH autofluorescence is most likely due to changes in the redox state of the coenzyme.[1,81] A loss in autofluorescence may suggest a concentration shift in the carcinogen-transformed cell's reduced NADH to the oxidized (and low quantum yield) NAD+. We note that in the studies reported here, data were collected on various proliferative states of both BEAS-2B and BEAS-2B$_{NNK}$ cells, with decreases similar to that shown in Figure 5 recorded for each state.

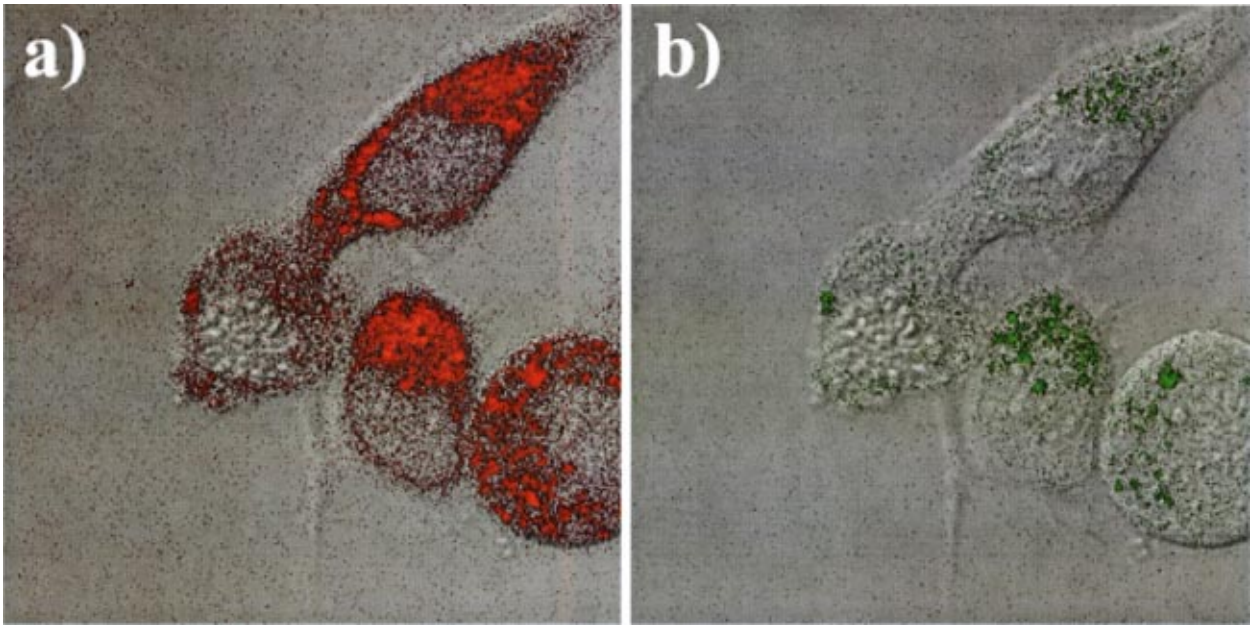

Fig. 4 Differential interference contrast images of immortalized human bronchial epithelial cells (BEAS-2B) with pseudocolor overlays of autofluorescence detected by confocal microscopy. (a) Cells were excited at 351 nm and the fluorescence emission was monitored between 426 and 454 nm. The granular, cytoplasmic autofluorescence detected (shown in red) corresponded closely to endogenous NADH. (b) The same cells were excited at 488 nm and the fluorescence emission was monitored between 530 and 555 nm. The granular, cytoplasmic autofluorescence detected (shown in green) corresponded closely to endogenous flavin emission. The cell on the left is in prophase of mitosis, as evidenced by the condensed chromosomes that are clearly visible.

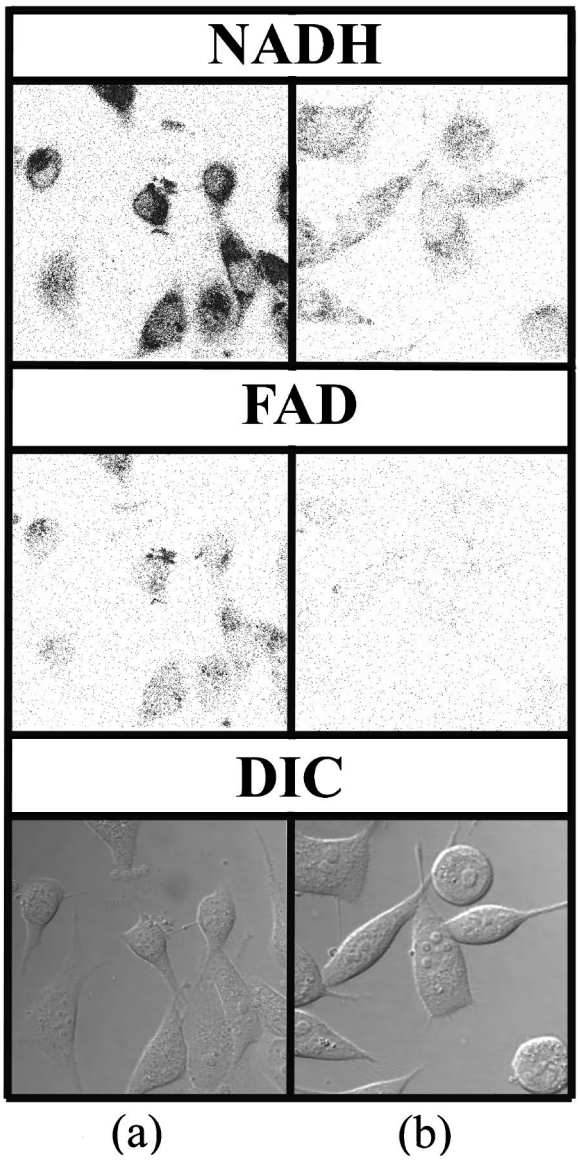

Fig. 5 Confocal autofluorescence microscopy images of (a) BEAS-2B and (b) BEAS-2B$_{NNK}$ cells. The top images show emission consistent with endogenous NADH. Relative to the BEAS-2B cells, a marked decrease was observed in the BEAS-2B$_{NNK}$ cells. Similarly, a loss in cytoplasmic granularity of the autofluorescence was observed. The middle images show emission consistent with endogenous flavins. A similar autofluorescence decrease was observed. The bottom figures show corresponding DIC images of each field.

In contrast to the observations reported above, a recent report compared steady-state and time-resolved autofluorescence in normal human bronchial epithelial (HBE) cells, non-metastatic, non-small cell lung cancer (NSCLC) cells, and metastatic small cell lung cancer (SCLC) cells.[70] The study found that NSCLC cells emitted more NADH and tryptophan fluorescence than normal HBE cells, while SCLC emitted more NADH fluorescence and similar levels of tryptophan fluorescence, when compared to normal HBE cells. It is important to point out that these measurements were reported on *one sample only* and were made at high cell counts using a spectrofluorimeter with front-face collection geometry. In our confocal fluorescence microscopy studies, we observed a consistent decrease in the carcinogen-transformed cell fluorescence versus immortalized cell fluorescence over many measurements using independent cellular cultures.

Finally, as seen in Figures 4 and 5(a), the BEAS-2B cells exhibit cytoplasmic, granular localization of the NADH fluorescence. This has been shown previously in a number of cell lines and was reported to be partially, but not totally, localized in the mitochondria.[42,44,82] It is interesting to note that granular cytoplasmic autofluorescence appeared less intense and less localized in the BEAS-2B$_{NNK}$ cells, relative to the BEAS-2B cells. A clear example is seen at the top of Figure 5(b). This loss of granular structure may be the result of changes in the mitochondrial morphology. A recent study noted that normal Galliera rat fibroblasts contain many filamentous mitochondria, while rat sarcoma lines contain a random cytoplasmic distribution of short spherical mitochondria.[44]

An appreciable reduction of the total flavin autofluorescence of the carcinogen-transformed human bronchial epithelial cells was also evident in Figure 5. A similar decrease in cellular flavin emission, from tumor human urothelial cells relative to normal human urothelial cells, was noted previously.[45] It was suggested, based on previous work,[79] that flavin fluorescence may be reduced in tumor cells, because deficient aerobic oxidation systems like tumors show reduced riboflavin concentrations. A second possible contributing factor may be redox changes similar to those hypothesized with NADH. Thus, biochemical pathways in the carcinogen-transformed cells may cause changes in the fluorescence by reducing FAD to the nonfluorescent $FADH_2$.[45,62] Our data are consistent with the observation of reduced total flavin emission in malignant versus normal cells.

These changes in cellular autofluorescence between immortalized and carcinogen-transformed human bronchial epithelial cells may indicate a potential method for noninvasively detecting pre-neoplasia in lung tissue using fluorescence spectroscopy and imaging. Much of the work on human bronchial tissue fluorescence[13–16,62,69] has revealed a consistent decrease in the autofluorescence of cancerous lesions versus normal bronchial tissue.[62] One cannot attribute all of the differences observed in tissues only to cellular fluorophores. Also contributing to measured tissue autofluorescence are fluorophores in the extracellular matrix, as well as morphological changes associated with pre-neoplastic tissue (including mucosal thickening and increased hemoglobin content) that are likely to influence light absorption and scattering. Nonetheless, the studies described here represent the first investigation of the autofluorescence properties of human bronchial epithelial cell lines that serve as model systems for neoplastic changes. By monitoring the changes in fluorescence emission from distinct fluorophores, such as NADH and flavins, or combinations of fluorophores, a sensitive and specific method for pre-neoplasia detection in the lung may be developed.

5 Conclusion

Using both spectrofluorimetry and confocal fluorescence microscopy, we characterized, for the first time, the spectral cellular autofluorescence properties of immortalized and distinct tobacco-carcinogen-transformed human bronchial epithelial

cells. Differences were observed between the two cell lines, as detected in confocal autofluorescence images that were specific to NADH and flavin emission. The observed loss in autofluorescence for carcinogen-transformed cells relative to immortalized bronchial epithelial cells may be the result of changes in fluorophore oxidation state. Future studies with improved sensitivity will seek to quantify both steady-state and time-resolved autofluorescence characteristics of these and other relevant cell lines, including chemoprevented cells and primary cultures of neoplastic cells.

Acknowledgments

The authors would like to thank Professor C. Braun for the use of his spectrofluorimeter and D. Sekula for cell preparation. The authors also wish to thank S. Honorowski, J. Montalvo, and A. Willson for technical assistance. This work was supported by Grant Nos. NSF MCB-9727818 (R.D.S.), NSF DBI-9970048 (R.D.S.), the American Society of Clinical Oncology (ASCO) Young Investigator Award (K.H.D.), Grant No. NIH RO1-CA87546 (E.D.), the Burke Research Initiation Award (M.A.M.), and Grant No. NSF BES-9977982 (M.A.M. and E.D.).

References

1. R. Richards-Kortum and E. Sevick-Muraca, ''Quantitative optical spectroscopy for tissue diagnosis,'' *Annu. Rev. Phys. Chem.* **47**, 555–606 (1996).
2. R. S. DaCosta, B. C. Wilson, and N. E. Marcon, ''Light-induced fluorescence endoscopy of the gastrointestinal tract,'' *Gastrointest Endosc* **10**(1), 37–69 (2000).
3. G. Wagnières, W. Star, and B. Wilson, ''*In vivo* fluorescence spectroscopy and imaging for oncological applications,'' *Photochem. Photobiol.* **68**(5), 603–632 (1998).
4. I. Bigio and J. Mourant, ''Ultraviolet and visible spectroscopies for tissue diagnostics: Fluorescence spectroscopy and elastic-scattering spectroscopy,'' *Phys. Med. Bio.* **42**, 803–814 (1997).
5. W. S. Glassman, C. H. Liu, G. C. Tang, S. Lubics, and R. R. Alfano, ''Ultraviolet excited fluorescence spectra from nonmalignant and malignant tissues of the gynecological tract,'' *Lasers Life Sci.* **5**, 49–58 (1994).
6. N. Ramanujam, A. Mahadevan, M. Follen-Mitchell, S. Thomsen, E. Silva, and R. Richards-Kortum, ''Fluorescence spectroscopy of the cervix,'' *Clin. Consult. Obstetrics Gynecol.* **6**(1), 62–69 (1994).
7. N. Ramanujam, M. Follen-Mitchell, A. Mahadevan, S. Thomsen, A. Malpica, T. Wright, N. Atkinson, and R. Richards-Kortum, ''Spectroscopic diagnosis of cervical intraepithelial neoplasia (CIN) *in vivo* using laser-induced fluorescence spectra at multiple excitation wavelengths,'' *Lasers Surg. Med.* **19**, 63–74 (1996).
8. N. Ramanujam, M. Follen-Mitchell, A. Mahadevan, S. Thomsen, A. Malpica, T. Wright, N. Atkinson, and R. Richards-Kortum, ''Development of a multivariate statistical algorithm to analyze human cervical tissue fluorescence spectra acquired *in vivo*,'' *Lasers Surg. Med.* **19**, 46–62 (1996).
9. N. Ramanujam, M. F. Mitchell, A. Mahadevan, S. Warren, S. Thomsen, E. Silva, and R. Richards-Kortum, ''*In vivo* diagnosis of cervical intraepithelial neoplasia using 337-nm-excited laser-induced fluorescence,'' *Proc. Natl. Acad. Sci. U.S.A.* **91**, 10193–10197 (1994).
10. M. A. D'Hallewin, L. Baert, and H. Vanherzeele, ''Fluorescence imaging of bladder cancer,'' *Acta Urol. Belg.* **62**(4), 49–52 (1994).
11. F. Konig, F. J. McGovern, A. F. Althausen, T. F. Deutsch, and K. T. Schomacker, ''Laser-induced autofluorescence diagnosis of bladder cancer,'' *J. Urol. (Baltimore)* **156**(5), 1597–1601 (1996).
12. M. Anidjar, O. Cussenot, S. Avillier, D. Ettori, P. Teillac, and A. LeDuc, ''The role of laser-induced autofluorescence spectroscopy in bladder tumor detection: Dependence on the excitation wavelength,'' in *Advances in Optical Biopsy and Optical Mammography*, R. R. Alfano, Ed., pp. 130–142, The New York Academy of Sciences, New York (1998).
13. S. Lam, J. Hung, and B. Palcic, ''Mechanism of detection of early lung cancer by ratio fluorometry,'' *Lasers Life Sci.* **4**(2), 67–73 (1991).
14. S. Lam, C. MacAulay, J. Hung, J. LeRiche, A. E. Profio, and B. Palcic, ''Detection of dysplasia and carcinoma *in situ* with a lung imaging fluorescence endoscope device,'' *J. Thorac. Cardiovasc. Surg.* **105**(6), 1035–1040 (1993).
15. S. Lam, C. J. Macaulay, C. Leriche, N. Ikeda, and B. Palcic, ''Early localization of bronchogenic carcinoma,'' *Diagnostic Therapeutic Endosc.* **1**, 75–78 (1994).
16. S. Lam, T. Kennedy, M. Unger, Y. E. Miller, D. Gelmot, V. Rusch, B. Gipe, D. Howard, J. C. LeRiche, A. Coldman, and A. F. Gazdar, ''Localization of bronchial intraepithelial neoplastic lesions by fluorescence bronchoscopy,'' *Chest* **113**(3), 696–702 (1998).
17. R. R. Alfano, G. Tang, A. Pradhan, M. Bleich, D. S. J. Choy, and E. Opher, ''Steady-state and time-resolved laser fluorescence from normal and tumor lung and breast tissues,'' *J. Tumor Marker Oncol.* **3**, 165–73 (1988).
18. G. C. Tang, A. Pradhan, and R. Alfano, ''Spectroscopic differences between human cancer and normal lung and breast tissues,'' *Lasers Surg. Med.* **9**, 290–295 (1989).
19. R. Cubeddu, A. Pifferi, P. Taroni, A. Torricelli, and G. Valentini, ''Noninvasive absorption and scattering spectroscopy of bulk diffuse media: An application to the optical characteristics of human breast,'' *Appl. Phys. Lett.* **74**(6), 874–876 (1999).
20. P. Gupta, S. Kumar Majumder, and A. Uppal, ''Breast cancer diagnosis using N2 laser-excited autofluorescence spectroscopy,'' *Lasers Surg. Med.* **21**, 417–422 (1997).
21. G. C. Tang, A. Pradhan, W. Sha, J. Chen, C. H. Liu, S. J. Wahl, and R. R. Alfano, ''Pulsed and cw laser fluorescence spectra from cancerous, normal, and chemically treated normal human breast and lung tissues,'' *Appl. Opt.* **28**(12), 2337–2342 (1989).
22. T. Vo-Dinh, M. Panjehpour, and B. Overholt, ''Laser-induced fluorescence for esophageal cancer and dysplasia diagnosis,'' in *Advances in Optical Biopsy and Optical Mammography*, R. R. Alfano, Ed., pp. 116–122, The New York Academy of Sciences, New York (1998).
23. T. Vo-Dinh, M. Panjehpour, B. Overholt, C. Farris, F. Buckley, and R. Sneed, ''*In vivo* cancer diagnosis of the esophagus using differential normalized fluorescence (DNF) indices,'' *Lasers Surg. Med.* **16**, 41–47 (1995).
24. M. Panjehpour, B. Overholt, T. Vo-Dinh, R. Haggutt, D. Edwards, and F. P. Buckley III, ''Endoscopic fluorescence detection of high-grade dysplasia in Barrett's esophagus,'' *Gastroenterology* **111**, 93–101 (1996).
25. M. Keijzer, R. Richards-Kortum, S. Jacques, and M. Feld, ''Fluorescence spectroscopy of turbid media: Autofluorescence of the human aorta,'' *Appl. Opt.* **28**(20), 4286–4292 (1989).
26. B. Chwirot, S. Chwirot, W. Jedrzejczyk, M. Jackowski, A. Raczynska, J. Winczakiewicz, and J. Dobber, ''Ultraviolet laser-induced fluorescence of human stomach tissues: Detection of cancer tissues by imaging techniques,'' *Lasers Surg. Med.* **21**, 149–158 (1997).
27. S. K. Majumder, A. Uppal, and P. K. Gupta, ''*In vitro* diagnosis of human uterine malignancy using N-2 laser-induced autofluorescence spectroscopy,'' *Curr. Sci.* **70**(9), 833–836 (1996).
28. Y. P. Sinichkin, S. R. Utz, A. H. Mavliutov, and H. A. Pilipenko, ''*In vivo* fluorescence spectroscopy of the human skin: Experiments and models,'' *J. Biomed. Opt.* **3**(2), 201–211 (1998).
29. Y. P. Sinichkin, S. R. Utts, I. V. Meglinskii, and E. A. Pilipenko, ''Spectroscopy of human skin *in vivo*: II Fluorescence spectra,'' *Mol. Spectrosc.* **80**(3), 383–389 (1996).
30. S. R. Utts, Y. P. Sinichkin, and E. A. Pilipenko, ''Laser fluorescence spectroscopy of human skin *in vivo*: The effect of erythema,'' *Opt. Spectrosc.* **76**(5), 771–774 (1994).
31. E. W. J. van der Breggen, A. I. Rem, M. M. Christian, C. J. Yang, K. H. Calhoun, H. J. C. M. Sterenborg, and M. Motamedi, ''Spectroscopic detection of oral and skin tissue transformation in a model for squamous cell carcinoma: Autofluorescence versus systematic aminolevulinic acid-induced fluorescence,'' *IEEE J. Sel. Top. Quantum Electron.* **2**(4), 997–1007 (1996).
32. K. Konig, A. Ruck, and H. Schneckenburger, ''Fluorescence detection and photodynamic activity of endogenous protoporphyrin in human skin,'' *Opt. Eng.* **31**(7), 1470–1474 (1992).
33. C. Kapadia, F. Cutruzzola, K. O'Brien, M. Stetz, R. Enriquez, and L. Deckelbaum, ''Laser-induced fluorescence spectroscopy of human colonic mucosa,'' *Gastroenterology* **99**, 150–157 (1990).
34. R. Cothren, R. Richards-Kortum, M. Sivak, M. Fitzmaurice, R. Rava,

G. Boyce, M. Doxtader, R. Blackman, T. Ivanc, G. Hayes, M. Feld, and R. Petras, ''Gastrointestinal tissue diagnosis by laser-induced fluorescence spectroscopy at endoscopy,'' *Gastrointest. Endosc.* **36**, 105–111 (1990).
35. K. T. Schomacker, J. K. Frisoli, C. C. Compton, T. J. Flotte, J. M. Richter, and T. F. Deutsch, ''Ultraviolet laser-induced fluorescence of colonic polyps,'' *Gastroenterology* **102**, 1155–1160 (1992).
36. K. T. Schomacker, J. K. Frisoli, C. C. Compton, T. J. Flotte, J. M. Richter, N. S. Nishioka, and T. F. Deutsch, ''Ultraviolet laser-induced fluorescence of colonic tissue: Basic biology and diagnostic potential,'' *Lasers Surg. Med.* **12**, 63–78 (1992).
37. R. Marchesini, M. Brambilla, and E. Pignoli, ''Light-induced fluorescence spectroscopy of adenomas, adenocarcinomas, and non-neoplastic mucosa in human colon 1. *In vitro* measurements,'' *J. Photochem. Photobiol., B* **14**, 219–230 (1992).
38. G. Bottiroli, A. C. Croce, D. Locatelli, R. Marchesini, E. Pignoli, S. Tomatis, C. Cuzzoni, S. DiPalma, M. Dalfante, and P. Spinelli, ''Natural fluorescence of normal and neoplastic human colon: A comprehensive ''*ex vivo*'' study,'' *Lasers Surg. Med.* **16**, 48–60 (1995).
39. Y. Yang, G. C. Tang, M. Bessler, and R. R. Alfano, ''Fluorescence spectroscopy as a photonic pathology method for detecting colon cancer,'' *Lasers Life Sci.* **6**(4), 259–276 (1995).
40. R. Cothren, M. Sivak, J. Van Dam, R. Petras, M. Fitzmaurice, and J. Crawford, ''Detection of dysplasia at colonoscopy using laser-induced fluorescence: A blinded study,'' *Gastrointest. Endosc.* **44**, 168–76 (1996).
41. M.-A. Mycek, K. Vishwanath, K. T. Schomacker, and N. S. Nishioka, ''Fluorescence spectroscopy for *in vivo* discrimination of premalignant colonic lesions,'' in *Biomedical Topical Meetings, OSA Technical Digest*, pp. 11–13, Optical Society of America, Washington, DC (2000).
42. J. E. Aubin, ''Autofluorescence of viable cultured mammalian cells,'' *J. Histochem. Cytochem.* **27**(1), 36–43 (1979).
43. K. Konig, H. Schneckenburger, A. Ruck, R. Steiner, and H. Walt, ''Laser-induced autofluorescence of cells and tissue,'' *Proc. SPIE* **1887**, 213–221 (1993).
44. A. C. Croce, A. Spano, D. Locatelli, S. Barni, and G. Bottiroli, ''Dependence of fibroblast autofluorescence properties on normal and transformed conditions. Role of metabolic activity,'' *Photochem. Photobiol.* **69**(3), 364–374 (1999).
45. M. Anidjar, O. Cussenot, J. Blais, O. Bourdon, S. Avrillier, D. Ettori, J.-M. Villette, J. Fiet, P. Teilllac, and A. LeDuc, ''Argon laser-induced autofluorescence may distinguish between normal and tumor human urothelial cells: A microspectrofluorimetric study,'' *J. Urol. (Baltimore)* **155**(5), 1771–1774 (1996).
46. P. Gedigk and E. Bontke, ''Detection of hydrolytic enzymes in lipopigments,'' *Z. Zellforsch Mikrosk Anat.* **44**, 495–518 (1956).
47. E. Essner and A. B. Novikoff, ''Human hepatocellular pigments and lysosomes,'' *J. Ultrastruct. Res.* **3**, 374–391 (1960).
48. A. N. Siakotos and K. D. Munkres, ''Recent developments in the isolation and properties of autofluorescent lipopigments,'' in *Ceroidlipofuscinosis*, N. K. D. Armstrong and J. A. Rider, Eds., pp. 167–178, Elsevier, New York (1982).
49. G. E. Eldred, G. V. Miller, W. S. Stark, and L. Feeney-Burns, ''Lipofuscin: Resolution of discrepant fluorescence data,'' *Science* **216**, 757–759 (1982).
50. J. R. Lakowicz, *Principles of Fluorescence Spectroscopy (Second Edition)*, 2nd ed., Kluwer Academic/Plenum, New York (1999).
51. W. Balcavage, ''On the fluorescence lifetime of tryptophan and proteins,'' *Photochemistry* **7**(3), 309–323 (1976).
52. R. F. Chen, ''Fluorescence quantum yields of tryptophane and tyrosine,'' *Anal. Lett.* **1**(1), 35–42 (1967).
53. A. Szabo and D. Rayner, ''Fluorescence decay of tryptophan conformers in aqueous solution,'' *J. Am. Chem. Soc.* **102**(2), 554–563 (1980).
54. J. C. Zhang, H. E. Savage, P. G. Sacks, T. Delohery, R. R. Alfano, A. Katz, and S. P. Schantz, ''Innate cellular fluorescence reflects alterations in cellular proliferation,'' *Lasers Surg. Med.* **20**, 319–331 (1997).
55. S. Ganesan, P. G. Sacks, Y. Yang, A. Katz, M. Al-Rawi, H. E. Savage, S. P. Schantz, and R. R. Alfano, ''Native fluorescence spectroscopy of normal and malignant epithelial cells,'' *Cancer Biochem. Biophys.* **16**, 365–373 (1998).
56. D. Parmeswarn, S. Ganesan, R. Nalini, P. Aruna, V. Veeraganesh, and R. R. Alfano, ''Native cellular fluorescence characteristics of normal and malignant epithelial cells from human larynx,'' *Proc. SPIE* **2979**, 759–764 (1997).
57. C. Brookner, M. Follen, I. Boiko, J. Galvan, S. Thomsen, A. Malpica, S. Suzuki, R. Lotan, and R. Richards-Kortum, ''Autofluorescence patterns in short-term cultures of normal cervical tissue,'' *Photochem. Photobiol.* **71**(6), 730–736 (2000).
58. D. L. Heintzelman, R. Lotan, and R. Richards-Kortum, ''Characterization of the autofluorescence of polymorphonuclear leukocytes, mononuclear leukocytes, and cervical epithelial cancer cells for improved spectroscopic discrimination of inflammation from dysplasia,'' *Photochem. Photobiol.* **71**(3), 327–332 (2000).
59. R. Richards-Kortum, C. Brookner, I. Boiko, A. Malpica, S. Thomsen, R. Lotan, and M. Follen, ''Biological basis of cervical tissue autofluorescence,'' in *Biomedical Topical Meetings, OSA Technical Digest*, pp. 209–211, Optical Society of America, Washington, DC (2000).
60. J. Qu, C. MacAulay, S. Lam, and B. Palcic, ''Optical properties of normal and carcinomatous bronchial tissue,'' *Appl. Opt.* **33**(31), 7397–7405 (1994).
61. R. R. Alfano, G. C. Tang, A. Pradhan, W. Lam, D. S. J. Choy, and E. Opher, ''Fluorescence spectra from cancerous and normal human breast and lung tissue,'' *IEEE J. Quantum Electron.* **23**(10), 1806–1811 (1987).
62. J. Hung, S. Lam, J. LeRiche, and B. Palcic, ''Autofluorescence of normal and malignant bronchial tissue,'' *Lasers Surg. Med.* **11**, 99–105 (1991).
63. T. Glanzmann, J.-P. Ballini, H. van den Bergh, and G. Wagnieres, ''Time-resolved spectrofluorometer for clinical tissue characterization during endoscopy,'' *Rev. Sci. Instrum.* **70**(10), 4067–4077 (1999).
64. H. Yokomise, K. Yanagihara, T. Fukuse, T. Hirata, O. Ike, H. Mizuno, H. Wada, and S. Hitomi, ''Clinical experience with lung-imaging fluorescence endoscope (LIFE) in patients with lung cancer,'' *J. Bronchol.* **4**, 205–208 (1997).
65. D. R. Doiron, A. E. Profio, R. G. Vinvent, and T. J. Dougherty, ''Fluorescence Bronchoscopy for detection of lung cancer,'' *Chest* **76**, 27–32 (1979).
66. A. E. Profio, D. R. Doiron, O. J. Balchum, and G. C. Huth, ''Fluorescence bronchoscopy for localization of carcinoma *in situ*,'' *Med. Phys.* **10**(1), 35–39 (1983).
67. A. E. Profio, D. R. Doiron, and E. G. King, ''Laser fluorescence bronchoscopy for localization of occult lung tumors,'' *Med. Phys.* **6**(6), 523–525 (1979).
68. S. Lam, C. MacAulay, and B. Palcic, ''Detection and localization of early lung cancer by imaging techniques,'' *Chest* **103**, 12S–14S (1993).
69. S. Lam, J. Hung, S. M. Kennedy, J. C. LeRiche, S. Vedal, B. Nelems, C. E. MacAulay, and B. Palcic, ''Detection of dysplasia and carcinoma *in situ* by ratio fluormetry,'' *Am. Rev. Respir. Dis.* **146**, 1458–1461 (1992).
70. A. Pradhan, P. Pal, G. Durocher, L. Villeneuve, A. Balassy, F. Babai, L. Gaboury, and L. Blanchard, ''Steady-state and time-resolved fluorescence properties of metastatic and nonmetastatic malignant cells from different species,'' *J. Photochem. Photobiol., B* **31**, 101–112 (1995).
71. R. Reddel, Y. K. Ke, V. Gerwin, M. McMenamin, J. Lechner, R. Su, D. Brash, J.-B. Park, J. Limb Rhim, and C. Harris, ''Transformation of human bronchial epithelial cells by infections by SV40 or adenovius-12 SV40 hybrid virus, or transfection via strontium phosphate coprecipitation with the plasmid containing SV40 early region genes,'' *Cancer Res.* **48**, 1904–1909 (1988).
72. J. Langenfeld, F. Lonardo, H. Kiyokawa, T. Passalaris, M. Ahn, A. Rusch, and E. Dmitrovsky, ''Inhibited transformation of immortalized human bronchial epithelial cells by retinoic acid is linked to cyclin E down-regulation,'' *Oncogene* **13**, 1983–1999 (1996).
73. J. Langenfeld, H. Kiyokawa, D. Sekula, J. Boyle, and E. Dmitrovsky, ''Post-translational regulation of cyclin D1 by retinoic acid: A chemoprevention mechanism,'' *Proc. Natl. Acad. Sci. U.S.A.* **94**, 12070–12074 (1997).
74. J. Boyle, J. Langenfeld, F. Lonardo, P. Reczek, V. Rusch, M. Dawson, and E. Dmitrovsky, ''Cyclin D1 proteolysis is a retinoid cancer chemoprevention signal in normal, immortalized, and transformed human bronchial epithelial cells,'' *J. Natl. Cancer Inst.* **91**(4), 373–379 (1999).
75. F. Lonardo, V. Rusch, J. Langenfeld, E. Dmitrovsky, and D. S. Klimstra, ''Overexpression of cyclins D1 and E is frequent in bronchial

preneoplasia and precedes squamous cell carcinoma development,'' *Cancer Res.* **59**, 2470–2476 (1999).
76. F. Jenkins and H. White, *Fundamentals of Optics*, McGraw-Hill, New York (1957).
77. I. D. Campbell and R. A. Dwenk, *Biological Spectroscopy*, Benjamin Cummings, Menlo Park, CA (1984).
78. P. G. Sacks, H. E. Savage, J. Levine, V. R. Kolli, R. R. Alfano, and S. P. Schantz, ''Native cellular fluorescence identifies terminal squamous differentiation of normal oral epithelial cells in culture: A potential chemoprevention marker,'' *Cancer Lett. (Shannon, Ireland)* **104**, 171–181 (1996).
79. M. A. Pollack, A. Taylor, J. Taylor, and R. J. Williams, ''Vitamins in cancerous tissues I. Riboflavin,'' *Cancer Res.* **2**, 739–745 (1942).
80. B. Chance and B. Schoener, ''Fluorometric studies of flavin component of the respiratory chain,'' in *Flavins and Flavoproteins*, E. C. Slater, Ed., Elsevier, New York (1966).
81. B. Chance, P. Cohen, F. Jobis, and B. Schoener, ''Intracellular oxidation-reduction rates *in vivo*. The microfluorometry of pyridine nucleotide gives a continuous measure of the oxidation state,'' *Science* **137**, 499–508 (1962).
82. H. Andersson, T. Baechi, M. Hoechl, and C. Richter, ''Autofluorescence of living cells,'' *J. Microsc.* **191**, 1–7 (1998).